Supplementary Figure 1. Alignment of hemagglutinin amino acids in H5N1 field strains and respiratory droplet transmissible variants

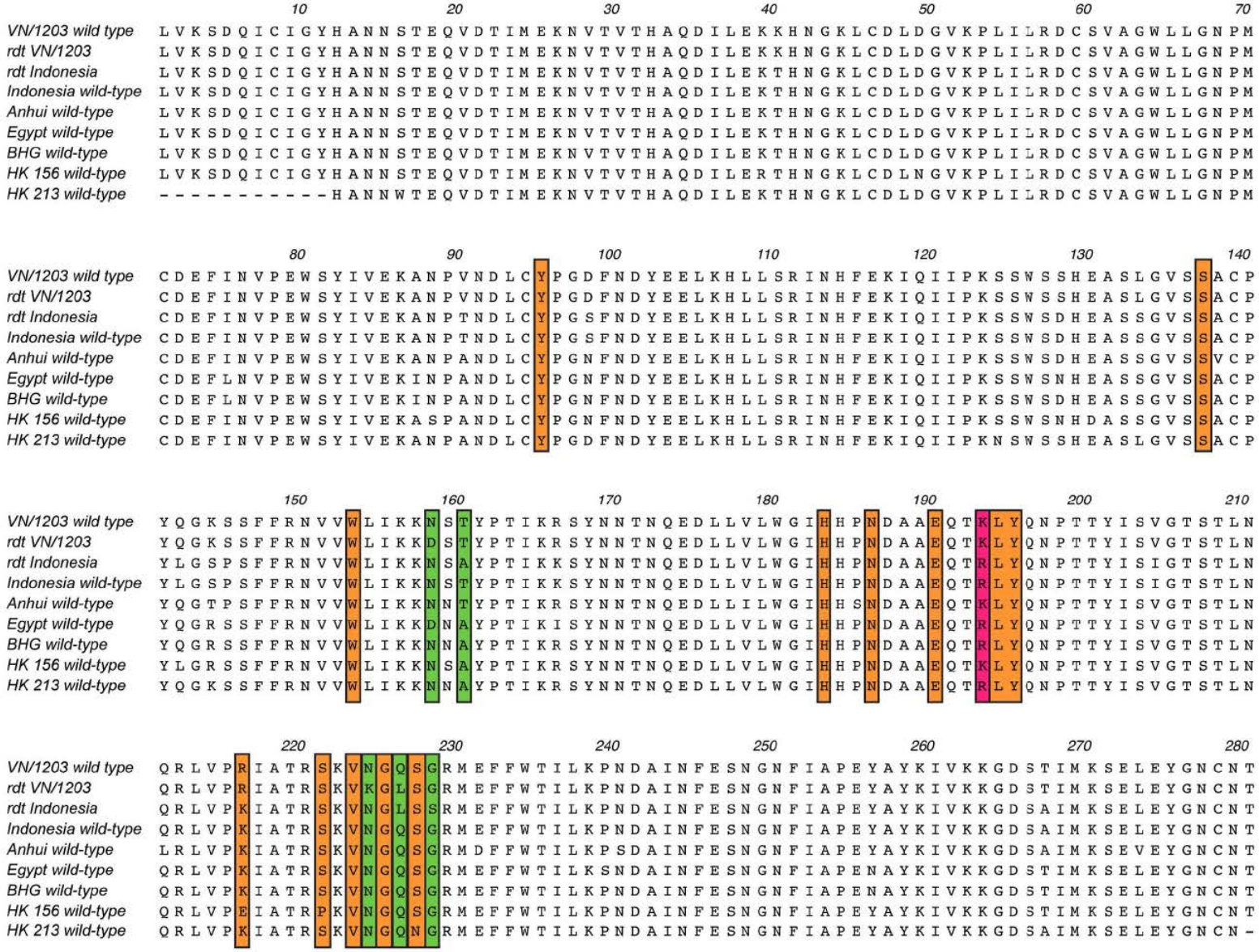

Partial HA sequences from H5N1 field variants and respiratory droplet transmissible variants are shown. Residues involved in receptor binding are highlighted in orange. Residues mutated in highly transmissible variants are highlighted in green. Residue 193 is highlighted in magenta.

Supplementary Figure 2. 16 Å Electron microscopy reconstruction of H5.3 Fab bound to the A/Vietnam/1203/2004 HA trimer.

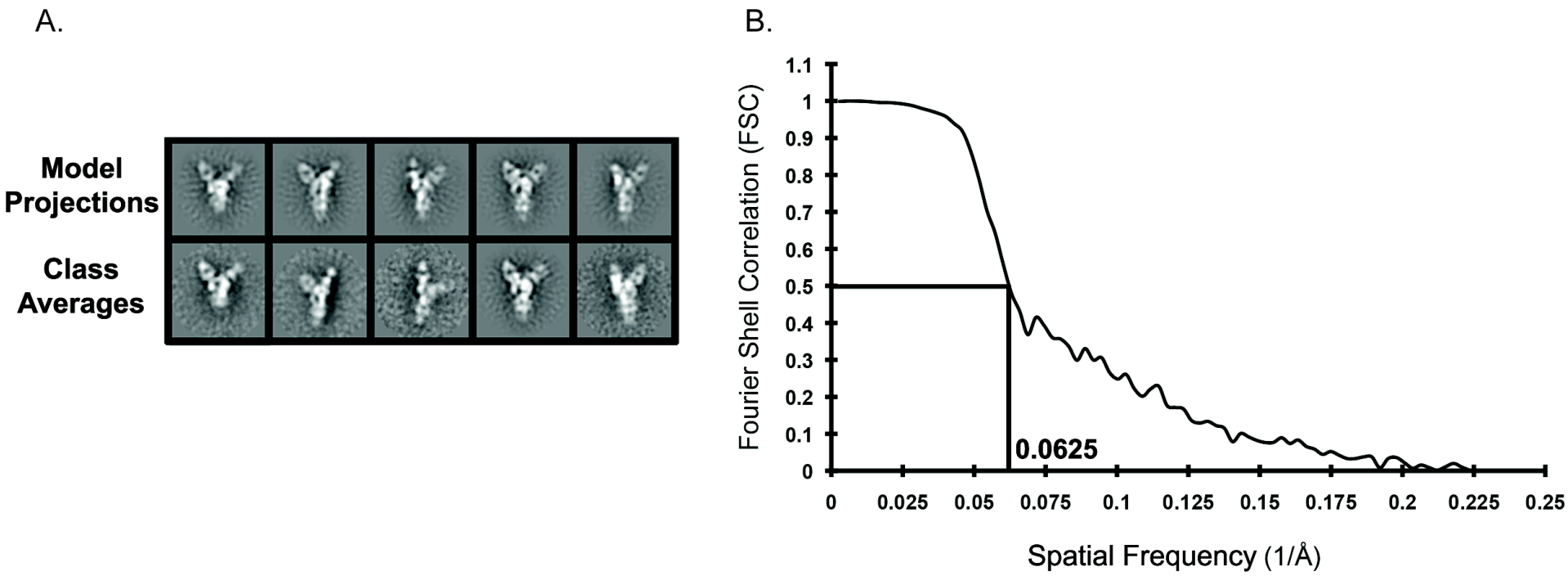

A density map of H5.3 Fab in complex with the A/Vietnam/1203/2004 HA trimer was determined by negative stain single-particle EM.

Panel A. Forward projections of the final reconstruction (top row) are shown in comparison to matching reference free class averages (bottom row).

Panel B. The resolution of the EM density was determined to be 16 Å by the Fourier Shell Correlation (FSC) curve at the FSC-0.5 cut-off.

Supplementary Figure 3. Computational modeling of mAb H5.3 complex with Vietnam/1203 HA.

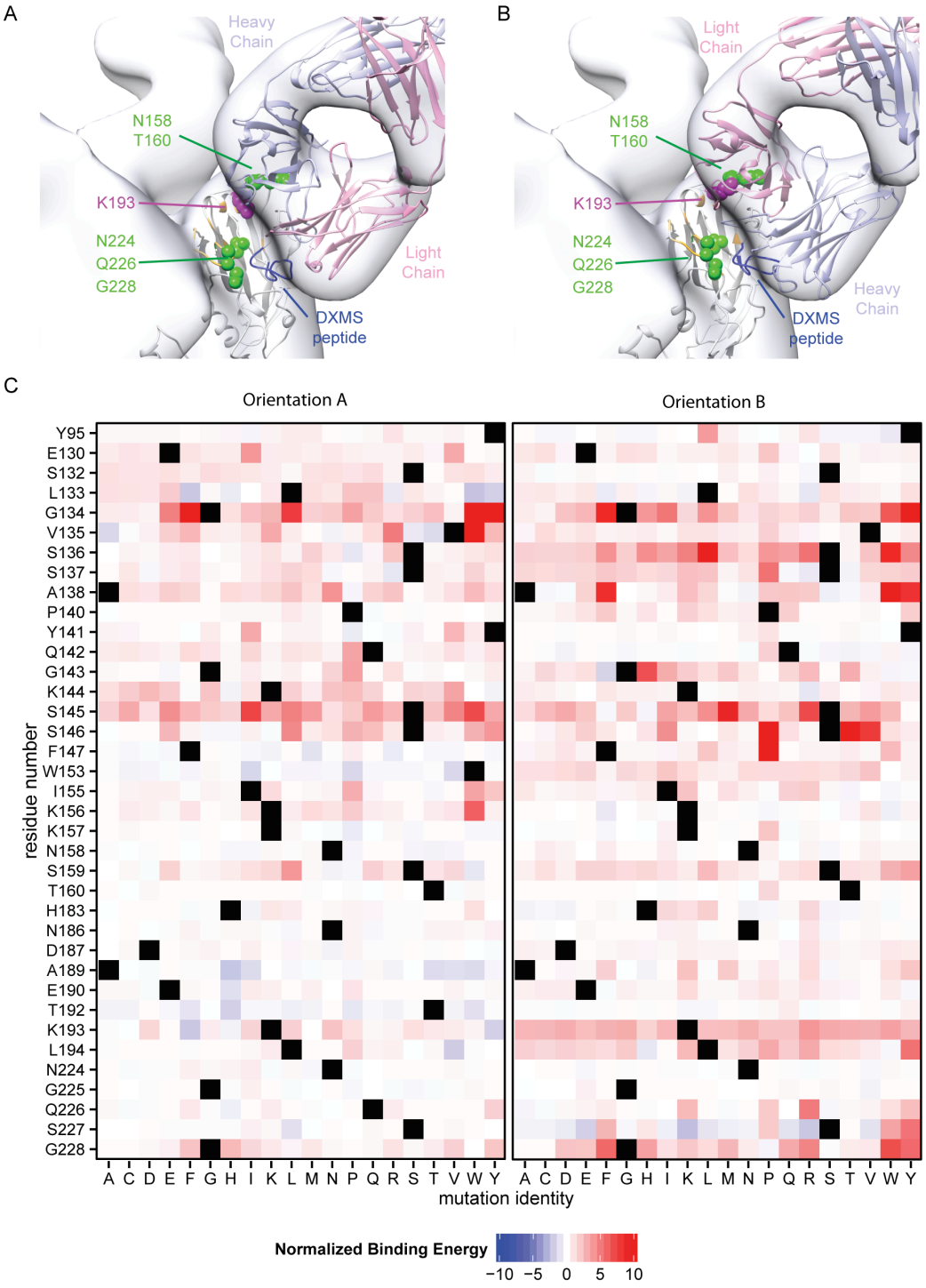

Docking was performed using atomic resolution structures of H5.3 Fab and the HA trimer of A/Vietnam/1203/2004 with Rosetta, as described in the detailed online methods. Because of the low resolution of the density map two possible orientations of the Fab were tested. Models for each are shown in A and B, with the better initial fit shown in Panel B (as in Figure 3 of the main text). Fab heavy chain (HC) is blue, Fab light chain (LC) is pink and H5 HA is gray. EM density is displayed as a transparent blue surface. *rdt* mutations are shown as green spheres, and the known escape mutation K193 colored purple. Important peptides in the DXMS analysis are colored blue. Measurement of the Fab correlation with the EM density map after fitting of the whole model indicated similar quality for each structure. C. Saturation mutagenesis of interface residues for prediction of mutations expected to abrogate binding. Predicted binding energies of each variant were normalized to the native binding energy. Native residues are shown as black boxes.

Supplementary Figure 4. H5.3 inserts HCDR3 into the receptor binding site like broadly neutralizing antibodies to other HA subtypes.

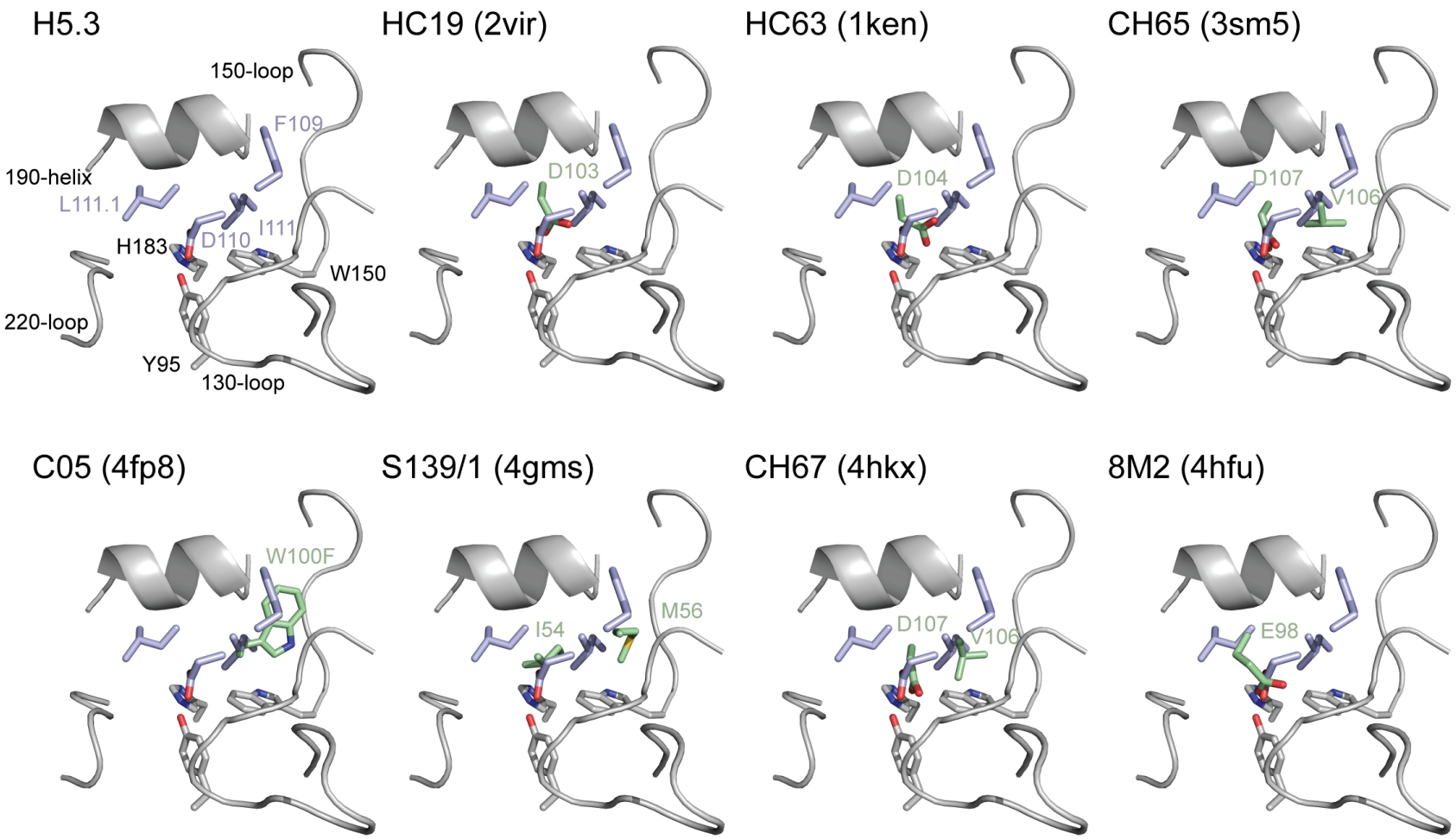

H5.3 uses a binding mode common to other influenza antibodies. In these panels, the HA receptor binding site-flanking 190 helix, 220 loop, and 130 loops are shown in grey (all panels). The mAb name is indicated for each structure; the PDB ID is shown for each in parenthesis. The HCDR3 side chains of H5.3 that reach into the receptor-binding site are show in blue (all panels). The blue H5.3 side chain are overlaid onto the HCDR3 of other broadly neutralizing antibodies from other HA subtypes, shown in green (29-35).

Supplementary Table 1. H5-specific human monoclonal antibodies (mAbs): Gene usage

Subject	mAb	Variable Gene Segments					Heavy chain CDR3 sequence	Heavy chain CDR3 amino acid length
		Heavy Chain			Light Chain			
		V_H	D	J_H	V_L	J_L		
18	H5.2	4-39*01	3-9*01	4*02	3-1*01	2*01	CARLSPNNILTGYYL	15
	H5.3	4-4*02	3-9*01	5*02	3-1*01	1*01	CARVALFDILTGGWFDPW	18
	H5.7	3-11*01	3-22*01	4*02	4-1*01	4*01	CARAGKSYDSSAFFDY	16
	H5.9	4-31*03	3-9*01	4*02	3-1*01	2*01	CARASPFNILIGYYFDYW	18
29	H5.13	1-24*01	3-10*01	6*02	1-39*01	1*01	CATDLMVRGLYYYGMDVW	18
	H5.16	1-8*01	3-3*01	5*02	3-11*01	2*01	CARGPERRTTIFDVILDWFDPW	22
42	H5.22	3-23*04	2-15*01	4*02	1-5*03	1*01	CAKESEIVVGYYFDYW	16
	H5.24	3-30-3*01	3-10*01	4*02	1-39*01	1*01	CARDVTSMIRGVSYFDYW	18
	H5.31	3-7*01	3-3*01	6*02	1-39*01	4*01	CARGFLERLLLGRQGAYYYGMDVW	22
54	H5.36	3-11*05	6-06*01	4*02	3-20*01	1*01	CARDEIYSSSRGGLDYW	17

Supplementary Table 2. Binding of human mAbs to HA molecules representing H5N1 virus *wt* field strains or variants

Domain / mAb		EC_{50} for binding to HA of indicated H5N1 strain [a] (ng/mL)											
		Wild-type H5N1 field strain							VN/1203 point mutant variant		Variants with *rdt* mutations in indicated *wt* virus background		
		VN/ 1203	Indo	Anhui	Egypt	BHG	HK/ 156	HK/ 213	K193S	K193R	*rdt* VN/ K[b]	VN/ F[c]	*rdt* Indo/ F
Head	H5.2	106	325	143	22	1,140	14	157	>	79	126	97	410*[d]
	H5.3	17	10,000	2,780	>[e]	>	18	>	>	>	19	16	>
	H5.9	200	1,800	376	178	16	22	61	21	28	137	192	>*
	H5.13	660	19,900	119	16	>	63	>	12,400	47	363	650	>
	H5.31	44	>	83	201	>	28	>	25	74	4	25	7
Stem	H5.7	79	156	134	12,800	518	109	275	111	193	8	34	18
nd [f]	H5.36	31	34	32	36	37	27	53	32	44	38	27	73

[a] Field strain HAs used were from A/Vietnam/1203/2004, clade 1.1 ("VN/1203"), A/Indonesia/05/2005, clade 2.1.3.2 ("Indo"), A/Anhui/1/2005, clade 2.3.4 ("Anhui"), A/Egypt/3300-NAMRU3/2008 ("Egypt"), A/bar-headed goose/Qinghai/1A/2005, clade 2.2.1.1 ("BHG"), A/Hong Kong/156/1997, clade 0 ("HK/156"), A/HK/213/2003, clade 0 ("HK/213"), A/Vietnam/1203/$2004_{N158D/N224K/Q226L}$ ("*rdt* VN/ K"), A/Vietnam/1203/$2004_{T160A,Q226L,G228S}$ ("VN/ F"), A/Indonesia/05/$2005_{T160A,Q226L,G228S}$ ("*rdt* Indonesia/ F")

[b] K [for Kawaoka strain] indicates N158D/N224K/Q226L mutations.

[c] F [for Fouchier strain] indicates T160A/Q226L/G228S mutations.

[d] * indicates EC_{50} differs from parental strain, as determined by non-overlapping 95% confidence intervals.

[e] > indicates a value of ≥ 50,000 was assigned when the curve did not reach a maximum within the limits of the assay.

[f] nd indicates domain *not determined* because of complex results in the functional mapping experiments.

Supplementary Table 3. H5.3 Fab crystal structure data collection and refinement statistics

Data collection	
Space group	$P6_1$
Cell dimensions	
a, *b*, *c* (Å)	150.43, 150.43, 70.517
Wavelength	0.97856
Resolution (Å)	50-2.25
Completeness (%)	50-2.25 Å: 99.7 (100)
Redundancy	50-2.25Å: 4.4(4.4)
I/sigmaI	50-2.25 Å: 18.3(2.6)
Refinement	
Resolution (Å)	2.25 Å
No. reflections	43,167
No. reflections free set	2,173
R_{work} / R_{free} %	17.23/20.31
R.m.s. deviations	
Bond lengths (Å)	0.008
Bond angles (°)	1.136
Ramachandran Plot	98.6% of residues in favored regions 0 outliers.

Supplementary Table 4. Predicted binding energy and experimental binding affinity for predicted escape or *rdt* point mutants

VN/1203 variant	Predicted binding energy (REU[a]) for indicated orientation		Experimental binding affinity (EC_{50}, μg/mL)
	Orientation A	Orientation B	
Wild-type (native)	-21.1 ± 0.2[b]	-26.6 ± 0.2	0.007
K193R	-20.7 ± 0.2	-22.7 ± 1.0	>[c]
K193S	-19.9 ± 0.3	-23.5 ± 0.2	>
N158D	-21.1 ± 0.2	-26.3 ± 0.2	0.007[d]
T160A	-21.2 ± 0.2	-26.7 ± 0.2	0.007[d]
N224K	-21.4 ± 0.2	-26.8 ± 0.2	0.007[d]
Q226L	-21.1 ± 0.4	-26.6 ± 0.2	0.007[d]
G228S	-21.1 ± 0.3	-26.8 ± 0.2	0.007[d]
V135I	-20.1 ± 0.2	-26.3 ± 0.3	0.056
S136R	-18.9 ± 0.3	-21.3 ± 0.1	>
S137A	-21.1 ± 0.2	-25.2 ± 0.2	0.007
G143H	-20.8 ± 0.3	-18.8 ± 1.5	>
S145L	-16.5 ± 0.8	-22.5 ± 0.2	>
K156R	-20.4 ± 0.6	-26.7 ± 0.2	0.031
A189T	-22.4 ± 0.1	-26.6 ± 0.3	0.007
A189Y	-21.5 ± 0.4	-24.7 ± 0.3	0.007
L194Y	-21.3 ± 0.4	-21.3 ± 0.6	0.187

[a] REU: Rosetta Energy Unit
[b] Mean and standard deviation of best 10 models
[c] > indicates a value of ≥ 10,000 was assigned when the curve did not reach a maximum within the limits of the assay.
[d] EC_{50} indicates binding comparable with wild-type H5.3. Mutants were tested experimentally in combination with associated *rdt* mutations.

SUPPLEMENTARY MATERIALS AND METHODS

Generation of human hybridomas secreting monoclonal antibodies (mAbs). Hybridomas were generated based on previously reported methods (1). Briefly, peripheral blood mononuclear cells (PBMCs) were isolated from blood from healthy adult donors who had participated previously in a Phase I clinical trial of an experimental H5N1 vaccine candidate in healthy adult subjects (DMID 04-062) (2). The vaccine was a monovalent inactivated subvirion vaccine prepared by Chiron Vaccines (now part of Novartis). The virus used to prepare the working seed and the vaccine was produced by reverse genetics using the modified hemagglutinin- and unaltered neuraminidase-encoding genes from the influenza A/Vietnam/1203/2004 (H5N1) strain and all other genes from A/Puerto Rico/8/34 (H1N1). PBMCs were transformed with Epstein Barr virus in the presence of Chk2 inhibitor (Sigma catalog no. C3742), cyclosporin A (Sigma) and CpG10103. The CpG10103 was synthesized as an oligonucleotide, TCGTCGTTTTTCGGTCGTTTT, containing phosphorothioate bonds (Invitrogen). The EBV-transformed cells were plated in 384-well microtiter plates and grown for 10 days, then screened by ELISA for binding to recombinant H5 hemagglutinin based on the sequence of the A/Vietnam/1203/2004strain. Cells from wells with supernatants containing antibodies that reacted with H5 HA in ELISA were collected, expanded by incubating in 96-well plates, and then fused with HMMA2.5 myeloma cells using a Cytopulse PA4000 electrofusion device. Hybridomas generated by this process were screened by ELISA, and those secreting antibodies binding to H5 HA were subcloned by limiting dilution.

Antibody gene cloning and sequence analysis. Antibody heavy and light chain variable genes were cloned by molecular means from each of the HA-reactive hybridomas lines that had been

cloned biologically by limiting dilution. Briefly, RNA was extracted using the RNeasy kit (Qiagen) and RT-PCR amplification of antibody gene cDNAs was performed using previously described primer sets (1). PCR products encoding lambda genes were cloned directly into the pGEM-T Easy kit (Promega), or additional rounds of PCR were performed for heavy chain or light chain genes to add DNA ends for subcloning into pGEM. The sequence of the antibody cDNAs was determined by automated sequencing techniques in the Vanderbilt University DNA sequencing facility. Nucleotide sequence determination and sequence analysis of variable gene sequences in the cDNAs was performed using the international ImMunoGeneTics information system (IMGT) (2). For variable genes that encoded unique sequences with in-frame open reading frames encoding antibodies, cDNAs were subcloned into an antibody expression plasmid system pEE12.4/pEE6.4 (Lonza).

Protein production. DNA copies of the genes encoding the hemagglutinin proteins of A/Vietnam/1203/2004, A/Anhui/1/2005 or A/Egypt/3300-NAMRU3/2008 were synthesized without the multi-basic cleavage site and subcloned into the pCDNA3.1+ mammalian cell expression vector (Invitrogen). Protein was expressed by transient transfection of 293F cells (Invitrogen) according to the manufacturer's instructions, with the exception that polyethyleneimine was used as the transfection reagent as previously described (3), instead of 293Fectin. Cells were grown for 7 days then harvested by centrifugation at 2500 x *g*. Supernatant was passed through a 0.45 μm membrane. The clarified supernatant was applied to a HisTrap HP column (GE Healthcare) Purified proteins were concentrated and buffer exchanged twice with DPBS using an Amicon Ultra centrifugal concentrator with a 10 kilodalton cutoff membrane (Millipore). Hemagglutinin proteins from A/Hong Kong/213/2003, A/Hong Kong/156/1997,

A/Indonesia/5/2005 and A/bar-headed goose/Qinghai/3/2005 were obtained from BEI Resources (Manassas, VA). For DXMS studies, a truncated monomeric A/Vietnam/1203/2003 HA head domain was expressed.

Antibodies used in the study were generated from hybridomas. Hybridomas were expanded and grown in serum-free medium (SFM, Invitrogen) as 1 L cultures. Cells were harvested when viability was less than 10%. Culture supernatants were prepared by centrifugation of cells and debris at 2,500 x *g* in a tabletop centrifuge for 20 minutes. The supernatant was passed through a 0.45 μm membrane and applied to a HiTrap Protein G HP column (GE Healthcare) Antibody sequences were checked for activity by expression of the recombinant antibody.

The subcloned antibody constructs were transfected into 293F cells using PEI as mentioned above and purified in the same manner as hybridoma-expressed antibodies.

Site-directed mutagenesis. The QuickChange II XL kit (Agilent) was used to generate HA constructs that possessed point mutations in the HA coding sequence of the plasmid encoding the A/Vietnam/1203/2004 HA. Mutagenesis was performed according to the manufacturer's instructions. The introduction of the intended mutation was confirmed by nucleotide sequence determination. All recombinant DNA protocols were approved by the Vanderbilt Institutional Biosafety Committee.

Viruses, and hemagglutination-inhibition and microneutralization assays. All functional assays were performed against influenza viruses reasserted with A/Vietnam/1203/2004 (H5N1)-PR8 virus or A/WSN/1933 (H1N1) grown in Madin Darby canine kidney cells (MDCKs).

Microneutralization assays were performed as described in Kong *et al.* (4). Briefly, two-fold serial diluted antibodies were tested in the presence of 100 $TCID_{50}$ virus on MDCK cell culture monolayers. After a two-day incubation period, cells were fixed and presence of viral nucleoprotein was determined by ELISA. Hemagglutination-inhibition assays were performed using standard procedures (4). Briefly, 4 hemagglutination units of virus was pre-incubated with two-fold dilutions of serially-diluted antibodies for one hour. Virus-antibody mixtures were incubated with turkey red blood cells (Innovative Research Inc.) for one hour at room temperature. The HI titer was defined as the highest dilution of antibody that inhibited hemagglutination of red blood cells.

Half maximal effective concentration (EC_{50}) binding analysis. HA proteins were coated onto immunoassay 384-well plates (Nunc) in DPBS at 1 μg/mL overnight, then antigen was removed and plates were blocked with 0.8% non-fat dry milk, 2% goat serum in PBS plus 0.1% Tween-20 for 30 minutes. Antibodies were applied in triplicate to the plates at a concentration range of 50 μg/mL – 0.64 ng/mL in block using five-fold serial dilutions. The presence of antibodies bound to HA was determined using anti-human IgG alkaline phosphatase conjugate (BioDesign) and p-nitrophenol phosphate substrate tablets (Sigma), with optical density read at 405 nM after 60 minutes. A non-linear regression analysis was performed on the resulting curves using Prism version 5 (GraphPad) to calculate EC_{50} values.

Pseudovirion production and neutralization assays. Lentiviral psuedovirions with wild-type, N158D/N224K/Q226L, or T160A/Q226L/G228S variant Vietnam/1203/HAs were produced in 293T cells, as previously described (5, 6). Briefly, plasmids pCMVdeltaR8.2 encoding HIV

Gag/Pol, Tat and Rev (Addgene) were co-transfected into 293T cells with pHR′CMV-GFP (Addgene), pCDNA3.1+ encoding human airway trypsin-like protease, and pCDNA3.1+ encoding with wild-type or *rdt* HA with Xtreme gene transfection reagent (Roche). At 24 hours post-infection, cells were washed and complete-medium was replaced with serum-free medium supplemented with 7 mU/mL of bacterial NA from *Vibrio cholera* (Sigma). At 42 hours post-transfection, supernatant containing pseudovirions was collected and cell debris was pelleted. Pseudovirions were treated with 10 μg/ mL TPCK trypsin (Sigma) for one hour at 37°C, trypsin was inactivated with 2% FBS, and pseudovirions were aliquoted and stored at -80°C. Neutralization assays were performed by pre-incubating pseudovirions with dilutions of antibodies containing 10 μg/ mL Polybrene (Millipore) for one hour at 37°C. Antibody-pseudovirion mixtures were used to spinoculate 293T cells at 800 rpm for 30 minutes. Titer was determined by counting GFP-positive cells at 72 hours post-spinoculation.

Biosensor assays. Antigen-antibody binding was confirmed by biosensor assays using Anti-Penta-HIS tips (ForteBio) with a factory-immobilized form of Qiagen's highly specific anti-His antibody or protein G tips on an Octet Red instrument (ForteBio). Stem- or head-binding phenotypes were confirmed by bioassay competitive binding assays using Ni-NTA tips (ForteBio). His-tagged A/Vietnam/1203/2004 HA was loaded onto Anti-Penta-His tips, and binding to two successive antibodies was tested. If binding of the first antibody blocked the binding of the second antibody, it was defined as a competitor. If binding of the first antibody did not block the binding of the second antibody, it was not defined as a competitor.

Crystallization and structure determination. H5.3 Fab crystals were grown by vapor diffusion of 21 mg/mL protein against a reservoir of 24% PEG 1500 and 20% glycerol. Crystals were frozen directly from the crystallization drops. Diffraction data were collected from single crystals at 100K at sector LS-CAT 21-ID-G at the Advance Photon Source (Argonne, IL). Data were indexed, integrated and scaled with HKL2000 (7). Data collection statistics are given in Supplementary Table 1 (Table S1). Molecular replacement was performed with Molrep (8) by iteratively searching a library of ~250 Fab fragments. The best solution, obtained with PDB 1FGW, was identified based on the Contrast score. Side chains of this oriented model that differed from the H5.3 sequence were trimmed to alanine, and the resulting oriented model was refined in Phenix (9). Refinement included rigid body refinement of the individual domains, simulated annealing, positional, individual B-factor, and TLS. Loops were rebuilt and side chains added in COOT (10) using simulated annealing composite omit maps (11) generated by Phenix (9). TLS refinement (12) was incorporated in the final rounds of refinement using TLS groups identified using Phenix. The refined model consists of amino acids 5-211 of the light chain, 2-223 of the heavy chain, and 188 water molecules. The final R_{factor} is 17.23%, the R_{free} is 20.31 for data between 50 and 2.25 Å. Additional data and model statistics are given in Table S1. The structure has been deposited in the Protein Data Bank under accession code 4GSD.

Electron microscopy and image processing. H5.3 Fabs were added to A/Vietnam/1203/2004 strain H5 HA trimer in six-fold molar excess and incubated at room temperature for 30 minutes. The complex was purified over Superose 6 size exclusion column (GE Healthcare) and concentrated to ~0.2 mg/mL. A 3 μL solution of 0.05 mg/mL complex was applied for 5 seconds onto a carbon coated Cu 400 mesh grid that had been glow discharged at 20 mA for 30 seconds,

then negatively stained twice with 2% uranyl formate. Data were collected using a FEI Tecnai F20 electron microscope operating at 120 keV using an electron dose of 20 $e^-/Å^2$ and a magnification of 100,000x that resulted in a pixel size of 1.09 Å at the specimen plane. Images were acquired with a Gatan 4k x 4k CCD camera using a nominal defocus range of 450 to 900 nm in 5° tilt increments from 0 to 55°.

Particles were picked automatically using DoG Picker and put into a particle stack using the Appion software package (13, 14). Initial reference free 2D class averages were calculated using particles binned by 4 via the Xmipp Clustering 2D Alignment (1, 15). Images of intact complexes were then selected and put into a substack. A template stack of 42 images of 2D class averages was used to generate 20 *ab initio* 3D models by EMAN2 and Sparx software packages. The model with the most clearly defined Fab and HA densities was used as the initial model for further refinement. Raw particle refinement was carried out using the substack, binned by 2, and by applying C3 symmetry for 99 iterations using the sxali3d.py program in the Sparx package (2, 16). The resolution of the final map from 5,721 particles is 16 Å as determined by an FSC cut-off of 0.5. The X-ray crystal structures of the trimeric H5 Vietnam HA (PDB ID: 2FK0) and H5.3 Fabs were fitted independently in two possible orientations in the electron density map using the Chimera 'Fit in map' function (1, 17). The orientation of the Fab displayed in Figure 1 was chosen because of its superior cross-correlation coefficient (0.895 vs. 0.869).

Peptide fragmentation and deuterium exchange. To maximize peptide probe coverage, the optimized quench condition was determined prior to deuteration studies (2, 18, 19). In short, 0.7 µL of stock solution of HA at 15 mg/mL was diluted with 7.3 µL of H_2O buffer (8.3 mM Tris, 150 mM NaCl, in H_2O, pH 7.15) at 0 °C and then quenched with 12 µL of 0.8% formic acid

(v/v) containing either 0.08M or 0.8M of GuHCl. The samples then were frozen on dry ice and stored at -80°C until they were transferred to the cryogenic autosampler.

The samples were later automatically thawed on ice and then immediately passed over an AL-20-pepsin column (16 μL bed volume, 30 mg/mL porcine pepsin (Sigma)), which was run at a flow rate of 20 μL/min with 0.05% trifluoroacetic acid. The resulting peptides were collected on a C18 trap and separated using a C18 reversed phase column (Vydac) running a linear gradient of 0.046% (v/v) trifluoroacetic acid, 6.4% (v/v) acetonitrile to 0.03% (v/v) trifluoroacetic acid, 38.4% (v/v) acetonitrile over 30 min with column effluent directed into an LCQ mass spectrometer (Thermo-Finnigan LCQ Classic). Data were acquired in both data-dependent MS:MS mode and MS1 profile mode. SEQUEST software (Thermo Finnigan Inc.) was used to identify the sequence of the peptide ions. DXMS Explorer (Sierra Analytics Inc., Modesto, CA) was used for the analysis of the mass spectra as described previously (3, 20). It was found that 0.08M GuHCl in 0.8% formic acid gave optimal peptide coverage map.

H5.3 - bound Vietnam/2003 HA were prepared by mixing H5.3 Fab with monomeric Vietnam/2003 HA head domain at 1:1.3 stoichiometric ratio. The mixtures were incubated at 0°C for 30 min. All functionally deuterated samples, with the exception of the equilibrium-deuterated control, and buffers were pre-chilled on ice and prepared in the cold room.

Functional deuterium-hydrogen exchange reaction of free Vietnam HA was initiated by diluting 0.7 μL of stock solution into 1.3 μL of H_2O buffer, and then mixed with 6 μL of D_2O buffer (8.3 mM Tris, 150 mM NaCl, in D_2O, pD_{READ} 7.15). At 10s, 100s and 1000s, 12 μL of optimized quench were added to their respective samples, and then samples were frozen at -80° C. The functionally deuterated antibody-bound HA samples were prepared by diluting 1.5 μL of complex solution (into 0.5 μL of non-deuterated buffer, and then mixed with 6 μL of D_2O buffer

(8.3 mM Tris, 150 mM NaCl, in D_2O, pD_{READ} 7.15). At 10s, 100s and 1000s, 12 μL of optimized quench were added to their respective samples, and then samples were frozen at -80°C.

In addition, non-deuterated samples (incubated in H_2O buffer mentioned above) and equilibrium-deuterated back-exchange control samples (incubated in D_2O buffer containing 0.5% formic acid overnight at 25°C) were prepared as previously described (4, 18, 19, 21). The centroids of the isotopic envelopes of non-deuterated, functionally deuterated, and fully deuterated peptides were measured using DXMS Explorer, and then converted to corresponding deuteration levels with corrections for back-exchange (4, 22).

Computational docking. Crystallographic coordinates for Vietnam/1203 H5 HA were obtained from the Protein Data Bank (2FK0, 3FKU and 3GBM) along with coordinates for the Fab H5.3 (PDB 4GSD). Each structure was minimized with eight rounds of the Rosetta FastRelax protocol. The full HA trimer was represented as a single protomer by making use of the symmetry functionality within Rosetta (5, 6, 23). Symmetry files were generated from the crystallographic HA trimer using the `make_symmfile.pl` script provided with Rosetta in the NCS mode. Harmonic restraints with a standard deviation of 0.5 were applied to all Cαs within an 8 Å radius and within a single HA protomer during the FastRelax protocol (7, 24). To consider possible conformational changes within HA or Fab upon binding, ensemble docking was employed. From the pool of relaxed HA structures a total of 30 were selected for docking simulations, the ten best scoring structures for each starting crystal structure. For the Fab the best scoring five structures were carried into docking. Each of these structures was superimposed with crystallographic structures that had been fit into the EM density map. Both possible orientations of H5.3 were tested. For each starting template 20 models were generated for a total of 6,000 models. Full

atom rigid body docking with side chain rotamer search was performed utilizing docking perturbations of 0.5 Å and 0.1° (8, 25). Restraints were generated from the DXMS data and applied during docking; these encouraged contact of residues 131-144 of HA with either the heavy or light chain of H5.3. Docking was performed with a single HA-Fab complex. A fully-bound trimeric HA was generated using the symmetry functionality (9, 26) for backbone and side chain minimization through eight rounds of FastRelax guided by the EM density map. Minimization was performed on the head domain of HA (residues 54-269) and the full Fab.

Models were evaluated for correlation with the EM density map, predicted binding energy and predicted binding density. For each antibody orientation, models which did not correlate well with the EM density map were pruned from the analysis and those models with a binding energy and binding density better than two standard deviations above the mean were carried forward. These models were analyzed for predicted effects on binding energy upon *in silico* generation of single mutants for which experimental binding data was available. A single model from each orientation which best represents this data was carried forward (Supplementary Figure 2). For each orientation, *in silico* saturation mutagenesis was performed on HA residues pointing toward the Fab and within 10 Å. Side chain atoms were replaced with the desired variant amino acid and the complex minimized through iterative side chain packing and gradient based minimization (27). Mutations were selected for experimental validation based on predicted change in binding energy and/or analysis of structural perturbation. A one-way ANOVA statistical analysis (GraphPad Prism 5) was performed to compare the sets of variants with EC50 of <1 μg/ml to variants with no detectable binding at 10 μg/mL. All Rosetta experiments were performed within the RosettaScripts framework with Rosetta3 r50946 (10, 28).

Rosetta command line for relax:

```
rosetta/rosetta_source/bin/rosetta_scripts.default.linuxgccrelease -s
PDB.pdb -parser:protocol symm_relax.xml -in:file:fullatom -
out:file:fullatom –database rosetta/rosetta_database/-linmem_ig 10 -
ex1 -ex2 -use_input_sc –nstruct 50 –relax:jump_move true
```

RosettaScripts XML script for relax (symm_relax.xml):

```
<ROSETTASCRIPTS>
   <SCOREFXNS>
      <score12_symm_cst weights=score12 symmetric=1 >
                        <Reweight scoretype=atom_pair_constraint
weight=0.5 />
      </score12_symm_cst>
   </SCOREFXNS>
   <TASKOPERATIONS>
      <InitializeFromCommandline name=ifcl />
      <RestrictToRepacking name=rtr />
      <IncludeCurrent name=ic />
   </TASKOPERATIONS>
   <FILTERS>
   </FILTERS>
   <MOVERS>
      <ConstraintSetMover name=cst cst_file=%%cst_file%% />
      <FastRelax name=relax scorefxn=score12_symm_cst repeats=8
task_operations=ifcl,rtr,ic />
      <SetupForSymmetry name=setup_symm definition=%%symm_file%% />
   </MOVERS>
   <APPLY_TO_POSE>
   </APPLY_TO_POSE>
   <OUTPUT scorefxn=score12_symm_cst />
   <PROTOCOLS>
      <Add mover=cst />
      <Add mover=setup_symm />
      <Add mover=relax />
   </PROTOCOLS>
</ROSETTASCRIPTS>
```

Example symmetry definition file:

```
symmetry_name HA_trimer
E = 3*VRT0_base + 3*(VRT0_base:VRT2_base)
anchor_residue COM
virtual_coordinates_start
```

```
xyz VRT0 -0.626193864858,-0.779667313754,0.000195603270636
0.779322401713,-0.625924347042,-0.0295850467323 -
0.0714551140462,0.559834809652,-14.6213399049
xyz VRT0_base -0.626193864858,-0.779667313754,0.000195603270636
0.779322401713,-0.625924347042,-0.0295850467323
10.6650705924,13.9277683953,-14.6246928502
xyz VRT1 0.987943369199,-0.152179839267,-0.0284458373982
0.152757074323,0.988074404607,0.0193455325729 -
0.0714551140462,0.559834809652,-14.6213399049
xyz VRT1_base 0.987943369199,-0.152179839267,-0.0284458373982
0.152757074323,0.988074404607,0.0193455325729 -
17.010424874,3.16906361838,-14.1336170494
xyz VRT2 -0.361749501941,0.931847252974,0.0282502360694 -
0.931837170019,-0.362342370204,0.0196843154662 -
0.0714551140462,0.559834809652,-14.6213399049
xyz VRT2_base -0.361749501941,0.931847252974,0.0282502360694 -
0.931837170019,-0.362342370204,0.0196843154662 6.13098893701,-
15.4173276847,-15.1057098172
xyz VRT 0.999471292597,-0.023571684522,-0.0223944404491
0.0240080036197,0.999523155577,0.0194184764628
0.928016178551,0.53626312513,-14.6437343454
virtual_coordinates_stop
connect_virtual JUMP0_to_com VRT0 VRT0_base
connect_virtual JUMP0_to_subunit VRT0_base SUBUNIT
connect_virtual JUMP1_to_com VRT1 VRT1_base
connect_virtual JUMP1_to_subunit VRT1_base SUBUNIT
connect_virtual JUMP2_to_com VRT2 VRT2_base
connect_virtual JUMP2_to_subunit VRT2_base SUBUNIT
connect_virtual JUMP0 VRT VRT0
connect_virtual JUMP1 VRT0 VRT1
connect_virtual JUMP2 VRT0 VRT2
set_dof JUMP0_to_com x(17.1456888058659)
set_dof JUMP0_to_subunit angle_x angle_y angle_z
set_jump_group JUMPGROUP2 JUMP0_to_com JUMP1_to_com JUMP2_to_com
set_jump_group JUMPGROUP3 JUMP1_to_subunit JUMP0_to_subunit
JUMP2_to_subunit
```

Rosetta command line for docking:

```
rosetta/rosetta_source/bin/rosetta_scripts.default.linuxgccrelease   -
database rosetta/rosetta_database/ -s   PDB.pdb -parser:protocol
dock_symm_min.xml -nstruct 20 -in:file:fullatom -out:file:fullatom -
linmem_ig 10 -docking:partners AB_HL -ex1 -ex2 -use_input_sc –
dock_mcm_trans_magnitude 0.5 –dock_mcm_rot_magnitude 0.1 –
```

```
relax:jump_move true –edensity:mapfile EMDENSITY.mrc –edensity:mapreso
16 –edensity:grid_spacing 6 –edensity:score_symm_complex –realign min
```

RosettaScripts XML script for docking (dock.xml):

```
<ROSETTASCRIPTS>
   <SCOREFXNS>
      <score12_symm_dens_cst weights=score12 symmetric=1 >
         <Reweight scoretype=atom_pair_constraint weight=0.5 />
         <Reweight scoretype=elec_dens_whole_structure_ca weight=0.01
/>
      </score12_symm_dens_cst>
   </SCOREFXNS>
   <TASKOPERATIONS>
      <InitializeFromCommandline name=ifcl />
      <RestrictToRepacking name=rtr />
      <IncludeCurrent name=ic />
   </TASKOPERATIONS>
   <FILTERS>
   </FILTERS>
   <MOVERS>
      <ConstraintSetMover name=cst cst_file=DXMS_cst.cst />
      <SetupForSymmetry name=setup_symm definition=%%symm_file%% />
      <FastRelax name=relax_iface scorefxn=score12_symm_dens_cst
repeats=8 task_operations=ifcl,rtr,ic >
         <MoveMap>
            <Span begin=1 end=50 chi=0 bb=0 />
            <Span begin=267 end=497 chi=0 bb=0 />
            <Span begin=51 end=266 chi=1 bb=1 />
            <Span begin=498 end=930 chi=1 bb=1 />
         </MoveMap>
      </FastRelax>
      <Docking name=docking jumps=1 local_refine=1 fullatom=1 design=0
conserve_foldtree=1 score_high=soft_rep ignore_default_docking_task=0
optimize_fold_tree=1 task_operations=ifcl />
   </MOVERS>
   <APPLY_TO_POSE>
   </APPLY_TO_POSE>
   <OUTPUT scorefxn=score12_symm_dens_cst />
   <PROTOCOLS>
      <Add mover=cst />
      <Add mover=docking />
      <Add mover=setup_symm />
      <Add mover=relax_iface />
   </PROTOCOLS>
```

```
</ROSETTASCRIPTS>
```

Rosetta command line for Mutational Analysis

```
rosetta/rosetta_source/bin/rosetta_scripts.default.linuxgccrelease
@mutant_analysis.flags -s PDB.pdb -parser:protocol mutant_analysis.xml
-nstruct 20 -parser:script_vars mut_pos=### mut_res=XXX
```

where ### and XXX represent the residue number and three letter code of the mutation.

RosettaScripts XML script for Mutational Analysis (mutant_analysis.xml)

```
<ROSETTASCRIPTS>
   <SCOREFXNS>
   </SCOREFXNS>
   <TASKOPERATIONS>
      <InitializeFromCommandline name=ifcl />
      <RestrictToRepacking name=rtr />
      <RestrictToInterfaceVector name=rtiv chain1_num=1,2
chain2_num=3,4 CB_dist_cutoff=10.0 nearby_atom_cutoff=5.5
vector_angle_cutoff=75 vector_dist_cutoff=9.0 />
      <DesignAround name=da_w_wt design_shell=1.0
resnums=1,190,186,219,134,136,164,225,223,221,155 repack_shell=1.5
allow_design=0 />
   </TASKOPERATIONS>
   <MOVERS>
      <MutateResidue name=mutate target=%%mut_pos%%
new_res=%%mut_res%% />
      <PackRotamersMover name=pack_mutation_sites scorefxn=soft_rep
task_operations=da_w_wt,rtr />
      <TaskAwareMinMover name=min_sc_mutation_sites tolerance=0.001
task_operations=da_w_wt,rtr type=dfpmin_armijo_nonmonotone chi=1 bb=0
jump=0 scorefxn=score12 />
      <PackRotamersMover name=soft_rp scorefxn=soft_rep
task_operations=rtiv,rtr,ifcl />
      <PackRotamersMover name=rp scorefxn=score12
task_operations=rtiv,rtr,ifcl />
      <TaskAwareMinMover name=soft_min tolerance=0.001
task_operations=rtiv type=dfpmin_armijo_nonmonotone chi=1 bb=1 jump=1
scorefxn=soft_rep />
      <TaskAwareMinMover name=soft_min_sc tolerance=0.001
task_operations=rtiv type=dfpmin_armijo_nonmonotone chi=1 bb=0 jump=0
scorefxn=soft_rep />
      <TaskAwareMinMover name=min_sc tolerance=0.001
task_operations=rtiv type=dfpmin_armijo_nonmonotone chi=1 bb=0 jump=0
scorefxn=score12 />
      <TaskAwareMinMover name=min tolerance=0.001 task_operations=rtiv
type=dfpmin_armijo_nonmonotone chi=1 bb=1 jump=ALL scorefxn=score12 />
```

```
      <ParsedProtocol name=minimize mode=sequence >
         <Add mover=soft_rp />
         <Add mover=soft_min_sc />
         <Add mover=soft_rp />
         <Add mover=soft_min />
         <Add mover=soft_rp />
         <Add mover=min_sc /><Add mover=soft_rp />
         <Add mover=min />
         <Add mover=rp />
         <Add mover=min_sc />
         <Add mover=rp />
         <Add mover=min />
      </ParsedProtocol>
      <InterfaceAnalyzerMover name=iface scorefxn=score12 packstat=0
pack_separated=1 fixedchains=A,B />
   </MOVERS>
   <FILTERS>
   </FILTERS>
   <APPLY_TO_POSE>
   </APPLY_TO_POSE>
   <PROTOCOLS>
      <Add mover=mutate />
      <Add mover=pack_mutation_sites />
      <Add mover=min_sc_mutation_sites />
      <Add mover=minimize />
      <Add mover=iface />
   </PROTOCOLS>
</ROSETTASCRIPTS>
```

SUPPLEMENTARY REFERENCES

1. Smith SA et al. Persistence of circulating memory B cell clones with potential for dengue virus disease enhancement for decades following infection. *J Virol*. 2012;86(5):2665–2675.

2. Brochet X, Lefranc M-P, Giudicelli V. IMGT/V-QUEST: the highly customized and integrated system for IG and TR standardized V-J and V-D-J sequence analysis. *Nucleic Acids Res*. 2008;36(Web Server issue):W503–8.

3. Durocher Y, Perret S, Kamen A. High-level and high-throughput recombinant protein production by transient transfection of suspension-growing human 293-EBNA1 cells. *Nucleic Acids Res*. 2002;30(2):E9–E9.

4. Kong W-P et al. Protective immunity to lethal challenge of the 1918 pandemic influenza virus by vaccination. *Proc Natl Acad Sci USA*. 2006;103(43):15987–15991.

5. McKay T, Patel M, Pickles RJ, Johnson LG, Olsen JC. Influenza M2 envelope protein augments avian influenza hemagglutinin pseudotyping of lentiviral vectors. *Gene Ther*. 2006;13(8):715–724.

6. Wang W et al. Establishment of retroviral pseudotypes with influenza hemagglutinins from H1, H3, and H5 subtypes for sensitive and specific detection of neutralizing antibodies. *J Virol Methods*. 2008;153(2):111–119.

7. Otwinowski Z, Minor W. Processing of X-ray diffraction data. *Methods in enzymology*. 1997;

8. Vagin A, Teplyakov A. MOLREP: an automated program for molecular replacement. *J Appl Crystallogr*. 1997;30:1022–1025.

9. Adams PD et al. PHENIX: building new software for automated crystallographic structure determination. *Acta Crystallogr D Biol Crystallogr*. 2002;58(Pt 11):1948–1954.

10. Emsley P, Cowtan K. Coot: model-building tools for molecular graphics. *Acta Crystallogr D Biol Crystallogr*. 2004;60(Pt 12 Pt 1):2126–2132.

11. Brünger AT, Adams PD, Rice LM. New applications of simulated annealing in X-ray crystallography and solution NMR. *Structure*. 1997;5(3):325–336.

12. Painter J, Merritt EA. Optimal description of a protein structure in terms of multiple groups undergoing TLS motion. *Acta Crystallogr D Biol Crystallogr*. 2006;62(Pt 4):439–450.

13. Voss NR, Yoshioka CK, Radermacher M, Potter CS, Carragher B. DoG Picker and TiltPicker: Software tools to facilitate particle selection in single particle electron microscopy. *J Struct Biol*. 2009;166(2):9–9.

14. Lander GC et al. Appion: An integrated, database-driven pipeline to facilitate EM image processing. *J Struct Biol*. 2009;166(1):95–102.

15. Sorzano COS et al. A clustering approach to multireference alignment of single-particle projections in electron microscopy. *J Struct Biol*. 2010;171(2):197–206.

16. Hohn M et al. SPARX, a new environment for Cryo-EM image processing. *J Struct Biol*. 2007;157(1):47–55.

17. Pettersen EF et al. UCSF Chimera--a visualization system for exploratory research and analysis. *J Comput Chem*. 2004;25(13):1605–1612.

18. Li S et al. Mechanism of intracellular cAMP sensor Epac2 activation: cAMP-induced

conformational changes identified by amide hydrogen/deuterium exchange mass spectrometry (DXMS). *J Biol Chem*. 2011;286(20):17889–17897.

19. Hsu S et al. Structural insights into glucan phosphatase dynamics using amide hydrogen-deuterium exchange mass spectrometry. *Biochemistry*. 2009;48(41):9891–9902.

20. Hamuro Y et al. Mapping intersubunit interactions of the regulatory subunit (RIalpha) in the type I holoenzyme of protein kinase A by amide hydrogen/deuterium exchange mass spectrometry (DXMS). *J Mol Biol*. 2004;340(5):1185–1196.

21. Lu WDW, Liu TT, Li SS, Woods VLV, Hook VV. The prohormone proenkephalin possesses differential conformational features of subdomains revealed by rapid H-D exchange mass spectrometry. *Protein Sci*. 2012;21(2):178–187.

22. Zhang Z, Smith DL. Determination of amide hydrogen exchange by mass spectrometry: A new tool for protein structure elucidation. *Protein Sci*. 2008;2(4):522–531.

23. Dimaio F, Leaver-Fay A, Bradley P, Baker D, André I. Modeling symmetric macromolecular structures in Rosetta3. *PLoS ONE*. 2011;6(6):e20450–e20450.

24. Kellogg EH, Leaver-Fay A, Baker D. Role of conformational sampling in computing mutation-induced changes in protein structure and stability. *Proteins*. 2011;79(3):830–838.

25. Chaudhury S et al. Benchmarking and analysis of protein docking performance in Rosetta v3.2. *PLoS ONE*. 2011;6(8):e22477.

26. Dimaio F, Tyka MD, Baker ML, Chiu W, Baker D. Refinement of protein structures into low-resolution density maps using rosetta. *J Mol Biol*. 2009;392(1):181–190.

27. Whitehead TA et al. Optimization of affinity, specificity and function of designed influenza inhibitors using deep sequencing. *Nat Biotechnol*. 2012;30(6):543–548.

28. Fleishman SJ et al. RosettaScripts: a scripting language interface to the Rosetta macromolecular modeling suite. *PLoS ONE*. 2011;6(6):e20161.

29. Bizebard T et al. Structure of influenza virus haemagglutinin complexed with a neutralizing antibody. *Nature*. 1995;376(6535):92–94.

30. Tsibane T et al. Influenza human monoclonal antibody 1F1 interacts with three major antigenic sites and residues mediating human receptor specificity in H1N1 viruses. *PLoS Pathog*. 2012;8(12):e1003067.

31. Ekiert DC et al. Antibody recognition of a highly conserved influenza virus epitope. *Science*. 2009;324(5924):246–251.

32. Whittle JRR et al. Broadly neutralizing human antibody that recognizes the receptor-binding pocket of influenza virus hemagglutinin. *Proc Natl Acad Sci USA*. 2011;108(34):14216–14221.

33. Ekiert DC et al. Cross-neutralization of influenza A viruses mediated by a single antibody loop. *Nature*. 2012;489(7417):526–532.

34. Lee PS et al. Heterosubtypic antibody recognition of the influenza virus hemagglutinin receptor binding site enhanced by avidity. *Proc Natl Acad Sci USA*. 2012;109(42):17040–17045.

35. Krause JC et al. Human monoclonal antibodies to pandemic 1957 H2N2 and pandemic 1968 H3N2 influenza viruses. *J Virol*. 2012;86(11):6334–6340.